

A new method to analyse species abundances in space using generalized dimensions

Leonardo A. Saravia*

Instituto de Ciencias Básicas, Universidad Nacional de General Sarmiento, J.M. Gutierrez 1159 (1613), Los Polvorines, Buenos Aires, Argentina

Summary

1. Species–area relationships (SAR) and species-abundance distributions (SAD) are among the most studied patterns in ecology, due to their application to both theoretical and conservation issues. One problem with these general patterns is that different theories can generate the same predictions, and for this reason, they cannot be used to detect different mechanisms of community assembly.
2. A solution is to search for more sensitive patterns, for example by extending the SAR to the whole SAD. A generalized dimension (D_q) approach has been proposed to study the scaling of SAD, but to date, there has been no evaluation of the ability of this pattern to detect different mechanisms.
3. An equivalent way to express SAD is the rank-abundance distribution (RAD). Here I introduce a new way to study SAD scaling using a spatial version of RAD: the species-rank surface (SRS), which can be analysed using D_q . Thus, there is an old D_q based on SAR (D_q^{SAD}), and a new one based on SRS (D_q^{SRS}). I perform spatial simulations to examine the relationship of D_q with SAD, spatial patterns and number of species. Finally, I compare the power of both D_q , SAD, SAR exponent and the fractal information dimension to detect different community patterns using a continuum of hierarchical and neutral spatially explicit models.
4. The SAD, D_q^{SAD} and D_q^{SRS} all had good performance in detecting models with contrasting mechanisms. D_q^{SRS} , however, had a better fit to data and allowed comparisons between hierarchical communities where the other methods failed. The SAR exponent and information dimension had low power and should not be used.
5. SRS and D_q^{SRS} could be interesting methods to study community or macroecological patterns.

Key-words: multifractals, multispecies spatial pattern, species–area relationship, species-rank surface

Introduction

The species–area relationship (SAR) is considered one of the oldest and best-documented patterns, and one of a few fundamental generalizations, in ecology (Crawley & Harral 2001; Šizling *et al.* 2011). The SAR is often characterized by a triphasic curve, with a range of intermediate scales corresponding to power-law relationship between the number of species and the area in which they occur (Preston 1960; Hubbell 2001). Although other quantitative forms could also be appropriate (Tjørve 2003; White *et al.* 2010), this power law is widely accepted (Rosindell & Cornell 2007) and implies a self-similar or fractal structure of species distributions for a community across spatial scales (Šizling & Storch 2004).

Species–area relationships only give information about the changes of richness with scale, but can be extended by incorporating the species-abundance distribution (SAD), using Hill's generalized diversity indices (Hill 1973), which follow from the definition of generalized entropies used in statistical

physics, called Renyi's entropies (Renyi 1970). The scaling exponents of Renyi's entropies are called generalized dimensions and are used in physics to characterize multifractals (Beck 1990). Multifractals and fractals are related techniques first used in physics to characterize scaling behaviour of complex structures (Stanley & Meakin 1988); the difference is that fractals look at the geometry of presence/absence patterns, while multifractals describe the arrangement of quantities such as population density or biomass (Saravia, Giorgi & Momo 2012a). Multifractal analysis has been applied to ecology in different areas: metapopulation models (Gamarra 2005), analysis of natural landscapes (Kirkpatrick & Weishampel 2005), search patterns in copepods (Seuront & Stanley 2014) and biomass dynamics in microalgae (Seuront & Spilmont 2002; Saravia, Giorgi & Momo 2012a; Dal Bello *et al.* 2014).

The application of generalized dimensions to extend SAR was first suggested by Ricotta (2000), and the methodology was later developed and applied to Barro Colorado Island forest plots by Borda-de-Água, Hubbell & McAllister (2002), who estimated generalized dimensions of SAD. Since then, several field studies have characterized species-abundance scaling – also called the species diversity–area relationship

*Correspondence author. lsaravia@ungs.edu.ar

(DAR) – using generalized dimensions and other multifractal techniques (Zhang *et al.* 2006; Yakimov *et al.* 2008; Wei *et al.* 2013). In addition, generalized dimensions have been applied to a spatially explicit neutral model (Yakimov *et al.* 2014a) and used in open source software for ecological multifractal analysis (Saravia 2014).

The SAD is another fundamental pattern in ecological communities and plays a major role in ecology and conservation (McGill *et al.* 2007). SADs have been used to compare different communities and to compare models and data, but is problematic because different mechanisms can produce nearly identical SADs (Chave, Muller-Landau & Levin 2002; Chisholm & Pacala 2010; Rosindell & Cornell 2013). SADs are often presented using rank-abundance diagrams (RADs) in which the log-abundance is plotted against the rank of the species (McGill *et al.* 2007). Rank-abundance diagrams are equivalent to cumulative distributions and thus a robust way to visualize the SAD without losing information (Newman 2005).

Here I propose a new way to analyse the relation of SAD with spatial scale, by attaching the rank of each species to its spatial distribution; in this way, the multivariate spatial distribution of species is summarized into a univariate two-dimensional distribution. I call this spatial distribution the species-rank surface (SRS), and it can be analysed and compared using generalized dimensions. This paper uses simulations of spatial patterns to compare the behaviour of generalized dimensions calculated from SRS and SAD. First, I use simple artificial spatial patterns: regular and randomized, combined with a uniform and logseries SAD, to observe the behaviour of generalized dimensions. Then, I use a continuum of neutral and hierarchical models to test whether generalized dimensions can detect different communities, estimating statistical power and type I error rate. I also compare the performance of generalized dimensions with single-dimensional indicators (the SAR exponent and the information dimension). A summary of the methods used to compare communities is presented in Table 1.

Table 1. Methods used to calculate the power to compare simulated communities with different degree of neutrality

Method	Name—meaning
SAD	Species-abundance distribution
D_q^{SAD}	Generalized dimension spectra based on SAD: characterize the scaling of species abundances in space
D_q^{SRS}	Generalized dimension spectra based on SRS: characterize the scaling of the spatial distribution of the ranks of species (SRS) derived from SAD
D_0^{SAD}	The power exponent of the species-area relationship. This is part of D_q^{SAD} and characterize the scaling of richness
D_1^{SRS}	Information dimension of SRS. This is part of D_q^{SRS} and characterize the scaling of Shannon diversity index calculated on the spatial distribution of species ranks

Methods

MULTIFRACTAL ANALYSIS

Extensive reviews of generalized dimensions and multifractal methods applied to ecology are available (Seuront 2009), and some good introductions have also been published (Scheuring & Riedi 1994; Borda-de-Água, Hubbell & He 2007); thus, I will only give a brief description. The generalized dimensions technique analyses the scaling properties of quantities distributed in a space that we assume to be two dimensional (i.e. a plane). This distribution should be self-similar across some range of scales, a property called multifractal, and can be mathematically represented in different ways (Harte 2001), of which the closest to ecology are the generalized dimensions D_q (Grassberger 1983), also called Renyi dimensions (Renyi 1970). D_q has been used to characterize the probabilistic structure of attractors derived from dynamical systems (Hentschel & Procaccia 1983).

I will analyse two kinds of D_q : the standard one used to analyse any quantity distributed in space, and another based on the SAD of a community in an area. The first kind is used to analyse the SRS (described later) and so is termed D_q^{SRS} . The second is based on SAD and named D_q^{SAD} . In both cases, I used the method of moments based on box counting (Evertsz & Mandelbrot 1992) to estimate generalized dimensions.

The mathematical representations for D_q^{SRS} and D_q^{SAD} are slightly different. For D_q^{SRS} the spatial distribution of quantities μ is covered with a grid, dividing it into $N(\epsilon)$ boxes of side ϵ , allowing us to calculate the value $\mu_i(\epsilon)$ in each. Then, the so-called partition function is computed as:

$$Z_q(\epsilon) = \sum_i^{N(\epsilon)} (\mu_i(\epsilon))^q, \tag{eqn 1}$$

where q can be any real number and is called *moment order*. The operation is performed for different values of ϵ and q , within a predetermined range. The generalized dimension is then calculated as:

$$D_q^{SRS} = \frac{1}{q-1} \lim_{\epsilon \rightarrow 0} \frac{\log(Z_q(\epsilon))}{\log \epsilon}. \tag{eqn 2}$$

When $q = 1$, the denominator of the first term in D_q^{SRS} is undefined, so it must be replaced by the following expression:

$$D_1^{SRS} = \lim_{\epsilon \rightarrow 0} \sum_i^{N(\epsilon)} \frac{\mu_i(\epsilon) \log(\mu_i(\epsilon))}{\log \epsilon}. \tag{eqn 3}$$

In practical cases as the limit cannot be assessed, and the dimensions are estimated as the slope of the $\log(Z_q)$ vs. $\log(\epsilon)$ in eqn 1 replacing by the numerator in eqn 3. This is done for different values of q , provided that it is a real number, which yields a graph of D_q^{SRS} in terms of q . This graph is called the spectrum of generalized dimensions.

To be an approximate multifractal, the relationship $\log(Z_q)$ vs. $\log(\epsilon)$ should be well described by a linear relationship, but a linear relationship with superimposed oscillations is also acceptable (Borda-de-Água, Hubbell & He 2007). A range of q and ϵ values must be established, and then D_q^{SRS} is estimated using linear regression. Note that D_q^{SRS} is defined as the limit $\epsilon \rightarrow 0$ (eqns 2 and 3), and thus, to use the method, it is sufficient that a scale exists below which a linear relationship applies (Hentschel & Procaccia 1983).

To analyse species-abundance–area relationships with multifractals using the method of Borda-de-Água, Hubbell & McAllister (2002), the boxes are replaced by species. Thus, at each spatial scale ϵ each species holds the quantity of interest: its own abundance. Then, the partition function is defined as a sum over the

species present $S(A)$ in an area A and the side of the box ε is replaced by the area:

$$Z_q(A) = \sum_i^{S(A)} (\mu_i(A))^q, \quad \text{eqn 4}$$

where $\mu_i(A)$ is the relative abundance of species i in an area A . D_q^{SAD} is defined as:

$$D_q^{\text{SAD}} = \frac{1}{1-q} \lim_{A \rightarrow \infty} \frac{\log(\langle Z_q(A) \rangle)}{\log A}. \quad \text{eqn 5}$$

The angle brackets indicate averages of $Z_q(A)$ over subplots with area A . Thus, when I calculate D_q based on SAD, I refer to it as D_q^{SAD} , and when I calculate D_q from the SRS, D_q^{SRS} ; D_q without a superscript refer to both.

D_q^{SAD} represents the scaling of the Hill's generalized diversity index (Hill 1973): when the moment order is $q = 0$, then D_q^{SAD} becomes the exponent of the SAR power-law scaling; when $q = 1$, D_q^{SAD} , represent the scaling of Shannon diversity index; and when $q=2$, D_q^{SAD} , becomes the scaling of Simpson's index. This is why D_q^{SAD} , can characterize DARs.

Theoretically D_q must be a non-increasing function of q (Hentschel & Procaccia 1983), which means that if $q_1 \geq q_2$ then $D_{q_1} \geq D_{q_2}$. Some studies have shown small violations of this property for D_q^{SAD} (Borda-de-Água, Hubbell & McAllister 2002; Zhang *et al.* 2006). These violations are related to the way that D_q^{SAD} is defined: the summation of eqn 4 is over species, while the summation of the original definition, eqn 1, is over boxes, and this changes the way in which the mathematical limits are taken and also the computation method of D_q^{SAD} . A partial solution has been proposed (Yakimov *et al.* 2014b), but the anomalies observed may be related to the mathematical assumptions needed for D_q to be non-increasing, in which case, a new mathematical proof should be developed for D_q^{SAD} . Thus, as long as the linear relationship is reasonable, I take D_q^{SAD} as a useful technique of analysis.

In a previous work, I proposed a new way to analyse species-abundance-area relationship using multifractals, one that fits more closely to the original definitions of eqns 1–3: the SRS (Saravia 2014). To construct the SRS, the spatial distribution of species has to be transformed by assigning to each species position its rank. First, I use the species abundances, at the whole plot level, to calculate the species' rank ordering from highest to lowest, assigning a number starting with one. If there are species with the same abundance, the ranks are assigned at random, and thus, all species are present in the surface. Then, the rank is assigned to the spatial position of the individuals of each species, forming a surface: a (mathematical) landscape with valleys formed by the most abundant species, and peaks determined by the rarest. Finally, the standard multifractal analysis is applied. If sampling was performed using quadrats, without taking the spatial position of individuals, the sum of the ranks of the species in the smallest quadrats can be used to form the SRS.

To determine whether a data set could be analysed using multifractals, there should be a linear relationship between $\log(Z_q)$ vs. $\log(\varepsilon)$, but oscillations might be present and the data sets still qualify as self-similar (Liebovitch 1998). For this reason, it is difficult to use tests of quadratic trends as proposed by Yakimov *et al.* (2008), because the curvature of a quadratic function can be fitted by a periodic function with the correct amplitude. To work around this problem, I used the coefficient of determination (R^2) as a measure of goodness-of-fit (Borda-de-Água, Hubbell & McAllister 2002); in general, this is not a good indicator of linearity, but since linearity is not exclusively required, I use it here in a descriptive way. The C++ source code to perform the multifractal analysis is available at <https://github.com/lisaravia/mfsba>.

To date, no theoretical shape of D_q has been derived for the spatial distributions of species; all that is known is that D_q is bounded such that D_∞ and $D_{-\infty}$ exist, and that D_q is a non-increasing function of q and thus that $D_{-\infty} \leq D_\infty$. Generalized dimensions (D_q) can be interpreted like a SAR power-law exponent: with larger values, the change in the number of species is greater when the scale of observation changes to a larger area. D_q expresses the change of the quantity under study when scale changes, but is modulated by q . When q is positive, the terms of the sums (eqns 2 and 5) with more abundant species have more weight and become even more important when q is greater. When q is negative, we have the opposite pattern: less abundant species have more weight in the sum, and so, D_q reflects the change of rare species. When $|q|$ is larger, D_q is driven by more and more extreme values, and thus, D_q will have higher variance because extreme values are rarer. Here I present most figures with a range of q from -24 to 24 , but for statistical comparisons, I use a smaller range (from -10 to 10) to avoid large variances.

Thus for negative q values (i.e. the left side of the curves in Fig. 2), D_q^{SAD} characterizes the scaling of less abundant species – but we do not know exactly which species, as the curvature of D_q^{SAD} when approaching $D_{-\infty}$ depends on the species abundances of the less abundant species, and we do not know exactly how the abundances and spatial patterns of these will influence the shape of D_q^{SAD} . D_q^{SRS} also reflect the spatial patterns of the less abundant species, and the quantity $D_{-\infty}$ can be independently calculated (Borda-de-Água, Hubbell & McAllister 2002) and used to study rare species from the point of view of SAD and SRS; this is a different possible application of generalized dimensions. The positive part of the D_q spectra characterizes the most abundant species for both SAD and SRS, but again it is unknown exactly how the shape of SAD, or its spatial pattern, will change the curvature of D_q . In this case the quantity D_∞ characterizes the most abundant species, and its relationship with $D_{-\infty}$ could give information about the relation of dominant and rare species. Thus, the range of D_q provides important information, but the shape of the spectrum is also necessary to characterize the scaling of SAD or SRS.

GENERALIZED DIMENSION RELATIONSHIP WITH SPATIAL PATTERNS AND SADS

I simulated species' spatial patterns with different SADs to demonstrate how D_q is related to them. First, I generated a uniform SAD, in which all species have approximately the same densities, by taking the number of individuals of each species from a Poisson distribution with the same mean. I distributed them in bands over a spatial grid, so they formed a regular spatial pattern, in which each grid position is occupied by exactly one individual. I chose the number of species to exactly divide the side of the grid, so all species are strips with approximately the same width (Fig. 1). I used square grids with sides of 256 and 512 sites containing 65 536 and 262 144 individuals, respectively, and 8, 64 and 256 species, and then calculated D_q for the regular pattern, randomizing the positions of species to compare D_q obtained with these two extreme cases. The second SAD used was a logseries (Fisher, Corbet & Williams 1943) with the same number of species and the same sides as above. I used the R package `untd` (Hankin 2007) to calculate the density for each species; this basically uses a Poisson distribution with the expected logseries abundances as means. I then built the regular pattern with strips of species, but as species have different abundances, the widths for each species are different (Fig. 1). I then estimated D_q for the regular and randomized patterns, simulated 10 spatial patterns for each case, and calculated the mean and standard deviation (SD) of D_q .

SPATIALLY EXPLICIT MODEL

To simulate more realistic patterns of species-abundance–area relationships, I used a stochastic spatially explicit model. For this, I developed a stochastic cellular automata (Molofsky & Bever 2004) model that can switch between neutral and hierarchical competition, representing a continuum between niche and neutral communities (Gravel *et al.* 2006). Under neutral competition individuals do not interact, and all have the same mortality, colonization rates and dispersal distances; in spite of these gross simplifications, neutral models are capable of predicting several real community patterns (Rosindell, Hubbell & Etienne 2011). At the other end of the continuum are niche communities represented by hierarchical competition models (Tilman 1994). In this case, species have differences that imply a competitive hierarchy, in which some species are always better than others, producing competitive exclusion (Chave, Muller-Landau & Levin 2002). I added a probability of replacement ρ to the neutral model: when $\rho = 1$ more competitive species always replace less competitive and the model behaves as a pure hierarchical one, and when $\rho = 0$, there is no replacement of species and the model is completely neutral. A more thorough description of the model is given in Appendix S1 (Supporting Information), and its C++ source code is available at <https://github.com/lasaravia/neutral> and figshare <http://dx.doi.org/10.6084/m9.figshare.969692>.

Following a classical neutral scheme, the model has a metacommunity: a regional collection of communities. With probability m , an individual of a species i can migrate from the metacommunity at a rate proportional to its frequency X_i in the metacommunity. Species can also disperse locally, and the model assumes an exponential dispersal kernel with average dispersal distance d . Other model parameters are the mortality rate μ , the number of species in the metacommunity and the size of the community, represented as the *side* of the grid used in the simulations. I used a logseries SAD for the metacommunity, defined by the maximum number of individuals ($side \times side$) and the number of species (Fisher, Corbet & Williams 1943). To represent a competition colonization trade-off, I chose the most competitive species to be less abundant in the metacommunity. Parameters values were in the range

estimated for BCI from the existing literature (Condit *et al.* 2002; Etienne 2007; Anand & Langille 2010).

I performed 50 simulations, with 500 time steps (Figs 1 & 2 in Appendix S2), for each combination of parameters given in Table 2. To compute the statistical power, I made comparisons of communities with different levels of ρ , representing more neutral or hierarchical communities, in which the other parameters were kept constant. I also made comparisons between repetitions with the same ρ to calculate the type I error.

STATISTICAL COMPARISON OF METHODS

I analysed the performance of two kinds of methods to differentiate communities. The first consists of a set of points or curves: SADs, generalized dimensions D_q^{SAD} and D_q^{SRS} . I am testing here for differences between two communities, thus I do not have information about the variability in D_q for each q or in abundance of each species, instead assuming that the sample comes from an unspecified univariate distribution. For these, I used a permutation procedure with the k -sample Anderson–Darling (AD) statistic (Scholz & Stephens 1987). The AD statistic measures the differences between the empirical distribution functions (EDFs) of two data sets as a weighted sum of square deviations between the EDFs (Feigelson & Babu 2012). This means that the information about q is lost, but as D_q spectrum is continuous and non-increasing – with the previously mentioned anomalies in D_q^{SAD} – the shape of the curve is mirrored in the EDF; this is why the method can be used. For SADs, the EDF is equivalent to the rank-abundance distribution (RAD) (Newman 2005), and thus, I am really comparing RADs with this method. I calculated p-values using 1000 permutations, in all cases using the package `kSamples` (Scholz & Zhu 2012) in the R statistical language (R Core Team, 2014). Scripts for all analyses are available at github <https://github.com/lasaravia/SpeciesRankSurface> and figshare <http://dx.doi.org/10.6084/m9.figshare.1276105>.

The second kind of comparison method is based on a single dimension or power exponent: the SAR exponent and the information

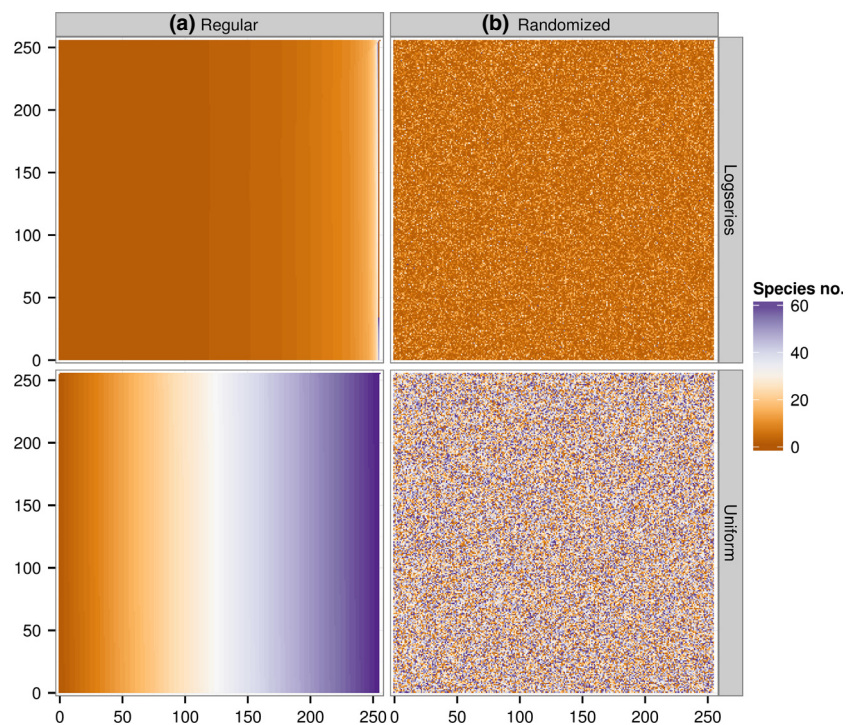


Fig. 1. Spatial patterns generated with log-series and uniform species-abundance distribution (all species have the same density) with 64 species and a grid with side = 256. (a) Regular: species are distributed in vertical bands. (b) Randomized: the position of species is distributed at random in space.

dimension. The SAR exponent is part of the D_q^{SAD} spectra when $q = 0$ (Borda-de-Água, Hubbell & McAllister 2002); an equivalent single number measure from D_q^{SRS} is the information dimension (Ricotta 2000; Chappell & Scalò 2001), that is the D_q^{SRS} when $q = 1$. I calculated the power of these with a t -test using the SD obtained from the box-counting regressions. These SD values are obtained with autocorrelated data, because small squares are nested within big squares (see Multifractal Analysis). The consequence is that the SD may be underestimated, but it has been shown that the slopes estimates are still unbiased (Kutner *et al.* 2005). This should result in an increased type I error rate and also in a spurious increase in statistical power. This power calculation, based on one dimension, should be lower than the power for the complete spectra, and I wanted to whether this simpler and less computationally intensive method give good results when comparing different communities. In at least some cases, autocorrelation does not have significant consequences (Legendre *et al.* 2002), and it is thus valuable to investigate the influence of autocorrelation in these single dimensions.

CALCULATION OF POWER AND TYPE I ERROR

I simulated communities with different degrees of neutral/hierarchical structure, given by the parameter ρ of the model. The power of a test is the ability to reject the null hypothesis (H_0) when false. The significance level to reject H_0 was set *a priori* at $\alpha = 0.05$ in all cases, and the rejection rate of each test was calculated as the proportion of P -values that less than or equal to α . To estimate power, I used independent simulations of communities (50 repetitions) with the same parameters except ρ .

The type I error is the probability of rejecting H_0 when it is true (false positive). In our simulations, H_0 is true if two simulated communities have the same ρ (and also are equal in the other parameters). To estimate type I error, I compared independent simulations of communities with the same set of parameters (50 repetitions) and computed the proportion of rejection.

Results

SIMPLE SPATIAL PATTERNS AND SAD

I calculated two versions of D_q : (i) the original definition due to Borda-de-Água, Hubbell & McAllister (2002), where D_q measures the change in SAD as we change scale (D_q^{SAD}), and (ii) D_q based on SRS, which measures the change in the spatial distribution of species' ranks as scale changes (D_q^{SRS}). D_q measures the rate of change with scale from a baseline that is defined by D_0 . When we study SAD, D_0^{SAD} is the SAR exponent and its value is around 0.5. A spatial distribution of species that duplicates its number with a duplication of the side of the area studied has a value of exactly 0.5. When we study SRS, the D_0^{SRS} is

Table 2. Parameters values used in the simulations of the neutral-hierarchical model

Side	No. species	μ	d	m	ρ
256	11	0.2	25	0.001	1
512	86				0.1
	341				0.01
					0.001
					0

the fractal dimension of the spatial distribution of species. Note that in the simulations here, the individuals completely fill the available space, and thus, D_0^{SRS} is equal to 2.

For the uniform SAD, we expected D_0^{SAD} to be around 0.5, following a symmetric pattern around $q = 0$, as all species have the same abundance and occupy the same area. The symmetric pattern was not observed in the regular cases (Fig. 2) because the negative part ($q < 0$) analyses numbers close to 0, and the logarithm (eqn 5) enhances the differences between small numbers (Laurie & Perrier 2011). Thus, the difference $\Delta D_q = |D_q - D_0|$ is greater for $q < 0$.

Theoretically, D_q should be decreasing or constant, but this was not observed in D_q^{SAD} for the randomized spatial patterns with few species. This is because when changing scales, there is a point at which no new species are found, and the scaling relationship breaks. Figure 3 shows the scaling of $Z_q(\epsilon)$ fitted using linear regression for 64 species and a side = 256 sites. The scaling for a randomized pattern D_q^{SAD} breaks at 1.2, equivalent to a box with side 16 or an area of 256 units. In contrast, the scaling for the regular pattern D_q^{SAD} shows oscillations around the fitted line but no evidence of breaks. When the number of species is high (256), the D_q^{SAD} is similar to the randomized one (Fig. 2); this happens because new species appear in the whole range of scales used.

The R^2 values (Table 1 in Appendix S2) indicate the presence of poor fits or a scaling break. The D_q^{SAD} for randomized patterns and uniform SAD have the lowest R^2 of all cases. Based on all simulations, I observe that the cases with the following conditions do not present anomalies: 90% of D_q should have an R^2 of 0.6 or greater, and 50% should have an R^2 of 0.9 or greater (Table 1 in Appendix S2); but one always should check the plots of the fits (Fig. 3) and eventually change the ϵ range. Several patterns fail to comply with these conditions: for example, all the uniform randomized patterns, and the logseries randomized with eight species (Table 1 and Figs 4–8 in Appendix S2), and these can be used as a guide to determine when the method can be applied.

The D_q^{SAD} for logseries had a more symmetric pattern than for uniform SAD (Fig. 2), and exhibited better fits with higher R^2 (Fig. 3). Comparing regular and randomized spatial patterns, the D_q^{SAD} curves were superimposed on, or inside, the SD of the other curve. Thus, it seems that D_q^{SAD} cannot distinguish between such patterns (although this only considers the cases with good fits). Moreover, the range of D_q^{SAD} did not change very much with the number of species, as D_q^{SAD} seems to depend mostly on the SAD used to generate the spatial pattern.

For D_q^{SRS} , the theoretical decreasing pattern was fulfilled in all cases, and no anomalies were observed (Fig. 2). As in the previous case, an asymmetrical pattern was observed with D_q^{SRS} around 2, an asymmetry more pronounced for patterns with uniform SAD than for logseries SAD. This is because logseries SAD have one very abundant species, with several less abundant and rare species scattered through the pattern (Fig. 1), and thus, the abundant species dominated the spatial pattern and in some cases produced a greater $\Delta D_q = |D_q - D_0|$ in the positive side of the plot (Fig 2, eight species).

The uniform SAD produced D_q^{SRS} with higher Δ_{Dq} values for regular patterns when $q < 0$. This is because the species are aggregated in the regular pattern, whereas in the randomized pattern, there is no aggregation, so D_q^{SRS} is closer to two. Thus, D_q^{SRS} for regular and randomized are more different on the negative side and more similar on the positive side. For log-series SAD, the differences in D_q^{SRS} are similar at negative or positive sides of q . In general, D_q^{SRS} curves for different spatial patterns and different SADs are distinct, except in some cases with 8 species, the curves for which are inside the SD of a different pattern.

The R^2 values for D_q^{SRS} were all >0.9 , higher than D_q^{SAD} , and all complied with the conditions described above (Table 1 in Appendix S2). Their linear trends were also better (Fig. 3). An example of linear trends for different number of species and different SADs is shown in the Figs 4–8 in Appendix S2. The same qualitative patterns of D_q^{SAD} and D_q^{SRS} were observed for simulations with side=512 (Fig. 1 in Appendix S2).

SIMULATED NEUTRAL COMMUNITIES

Examples of the patterns simulated by the neutral/hierarchical model are shown in Fig. 4. By definition, hierarchical communities have more competitive species with lower index numbers, and neutral communities have more abundant species with higher index numbers, as determined by metacommunity abundance (see Methods and model description in the Appendix S1). With a greater degree of competitive hierarchy, one or

few species dominate and several rare species are scattered over the landscape (Fig. 5). This produces a mostly uniform pattern of dominant species with rare species distributed at random. In neutral communities, the most abundant species are not so dominant (Fig. 5) and leave space for species with intermediate abundances, producing a pattern of several aggregated species. Aggregation is produced in this model only because dispersal is mainly near the parent.

For both estimated D_q the R^2 values were very good: D_q^{SRS} was always $R^2 > 0.9$ and D_q^{SAD} had in almost all cases $R^2 > 0.6$ and a 50% or more of the cases greater than 0.9 (Table 2 in Appendix S2). Figure 6 shows an example of D_q fitted using linear relationships for a metacommunity of 86 species and a side of 256 sites; examples with different metacommunity species and side values are given in Figs 9–13 in Appendix S2.

There are two groups of D_q^{SAD} (Fig. 7): one composed of neutral-like communities for $\rho < 0.1$ and another of more hierarchical communities for $\rho > 0.1$. The curves for hierarchical communities were more separated for negative q than for positive q , whereas this pattern was inverted in neutral communities, with positive q having more different curves. This reflects the patterns in SAD: hierarchical communities have one or few relatively abundant species, resulting in D_q^{SAD} reaching 0 quickly, and no new abundant species are found when changing scale. Neutral communities have more species with intermediate densities, producing $D_q^{\text{SAD}} > 0$ on the positive side.

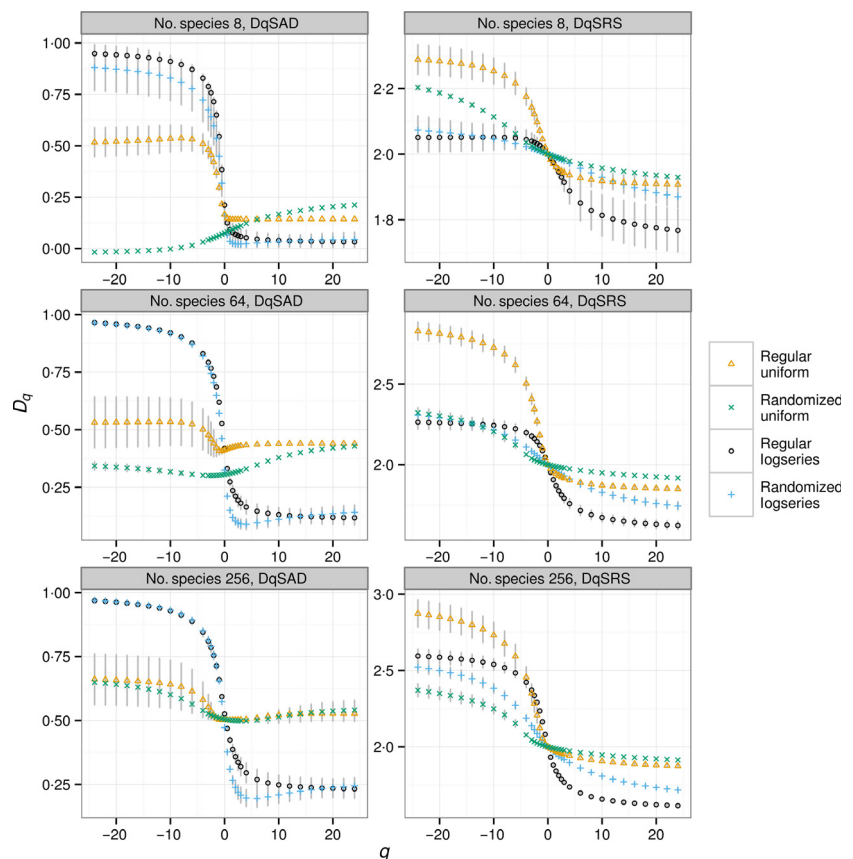


Fig. 2. Generalized dimension spectra D_q of simulated species spatial patterns. The points are means of 10 simulated patterns using a spatial grid of side = 256. A logseries or uniform species-abundance distribution (SAD) was used, with 8, 64 and 256 species. Two forms of generalized dimensions were estimated: DqSRS, from species-rank surface D_q^{SRS} . DqSAD, estimated from SAD D_q^{SAD} . I use two spatial patterns: regular, the species are distributed in vertical bands; randomized, the spatial distribution of species was randomized.

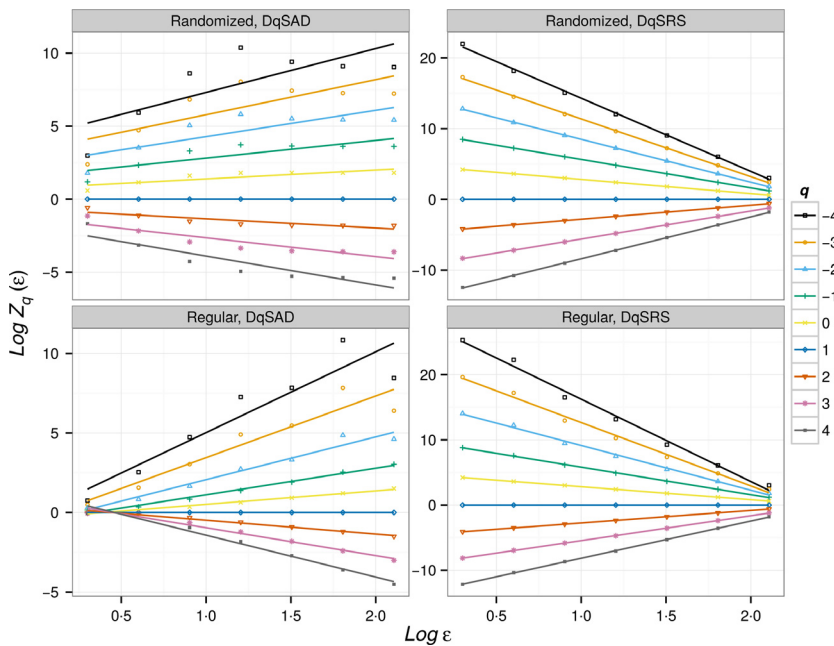


Fig. 3. Linear fit of $Z_q(\epsilon)$ to estimate generalized dimensions (D_q) from simple species spatial patterns with 64 species and a uniform-abundance distribution. The spatial grid has a side = 256 sites and two different spatial patterns: regular, a regular spatial pattern with species distributed in vertical bands of equal width; randomized, the positions of species in the grid are randomized. Two kinds of generalized dimension were estimated: DqSRS corresponds the fit of D_q^{SRS} (see text), and DqSAD is the fit from the estimation of D_q^{SAD} (see text). $Z_q(\epsilon)$ corresponds to the partition function calculated for a box with side ϵ , q is the moment order.

In theory, D_q have a constant value when q tends to infinity (negative or positive). Here, D_q^{SAD} spectra quickly reached a constant maximum for negative q and a minimum for positive q . This pattern was more pronounced with hierarchical communities, which tended to have dominant species reflected on the positive side, and rare species on the negative. When communities are more neutral ($\rho < 0.1$) and there are more species with intermediate densities, D_q^{SAD} tended to reach the asymptotic values more slowly in the negative side.

For D_q^{SRS} , similar groups of neutral or hierarchical communities were also present (Fig. 7). We previously saw that D_q^{SRS} is more related to the spatial pattern than is D_q^{SAD} , and thus, we can interpret D_q^{SRS} in terms of randomness and aggregation of species. For hierarchical communities, negative-side D_q^{SRS} is very close to 2, that is the dimension of a uniform surface, with rare species exerting a very low influence on uniformly distributed dominants. For neutral communities, there are more species with low to medium densities, with greater aggregation, and thus, D_q^{SRS} is higher.

When q is positive, lower values of D_q^{SRS} mean more-intense spatial patterns. Communities with $\rho = 1$ are the most hierarchical, with one dominant species and a few very rare species (Fig. 6). For these communities, D_q^{SRS} is closer to 2, representing the uniform spatial distribution of dominant species. When the metacommunity has more species, the local community also has more species (Table 3 in Appendix S2) and D_q^{SRS} starts to deviate from 2 at lower q . D_q^{SRS} for the intermediate hierarchical case ($\rho = 0.1$) starts higher than neutral at q near 0, but crosses neutral curves and ends in the lowest place. The communities have more species that also are more abundant, but still have few individuals; this forms very sharp peaks in the SRS and produces a D_q^{SRS} farther from 2. The curvature of D_q^{SRS} is thus more pronounced when there are more species. For ρ less than 0.1, communities are more neutral and have more species with

similar densities, forming softer valleys and peaks that result in a D_q^{SRS} intermediate between the two hierarchical cases. Simulations with side = 512 exhibited similar patterns for D_q (Fig. 14 Appendix S2).

STATISTICAL POWER AND TYPE I ERRORS

To calculate the power of the methods, I compared communities with different ρ values; in this comparison, the alternative hypothesis is true. Instead for estimating type I error, we need to compare different runs of communities simulated with identical parameters. I talk of high power when its value is 0.75 or higher, and low power when it is 0.5 or lower.

For D_q^{SAD} and D_q^{SRS} different ranges of q can be used. High values of q in absolute terms should produce D_q with high variances, resulting in a higher spread of values obtained in different simulation runs. Ranges of q between -10 and 10 or narrower are generally used (Yakimov *et al.* 2008; Laurie & Perrier 2011; Saravia, Giorgi & Momo 2012b; Wei *et al.* 2013), but sometimes the applied range has been wider (Saravia, Giorgi & Momo 2012a). I started using a q range of -24 to 24 and found that for this range type I error rates were, in all cases, higher than the nominal significance level $\alpha = 0.05$ (Table 4 in Appendix S2). As a statistical test is valid if the type I error is lower or equal to α (Edgington 1995), to assure the validity for these methods a narrower range should be used. I thus used a q range between -10 and 10 .

Using only one dimension of the spectra (D_0^{SAD} and D_1^{SRS}) resulted in a power generally below 0.5 (Table 3) and a type I error around 0.4. These high type I error values, much greater than α , were expected due to the presence of spatial autocorrelations in the dependent variable (Legendre *et al.* 2002). Parameter estimates can be corrected in different ways (Legendre *et al.* 2002), but these procedures should not increase the power of D_0^{SAD} and D_1^{SRS} .

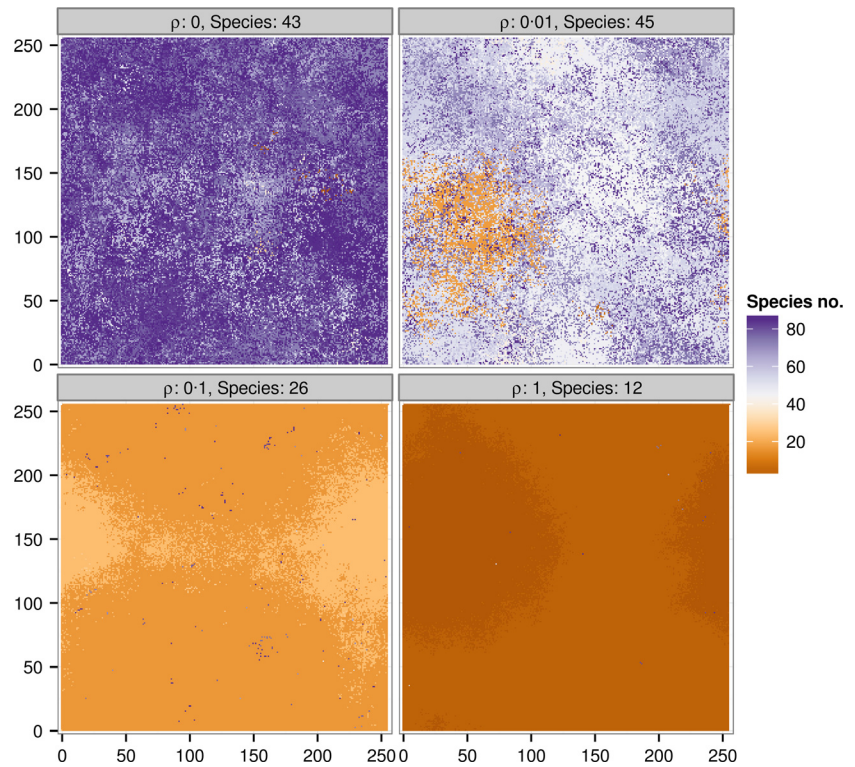


Fig. 4. Spatial patterns generated with a spatial neutral/hierarchical model. Rho (ρ) is the parameter that determines the degree of neutrality. When this parameter is 0, the model is completely neutral and there is no competitive replacement of species. When ρ is 1, competitive superior species always replaces inferior ones and the model is completely hierarchical. The Species number showed in each panel is the number of species actually present in the spatial patterns. The simulations use a metacommunity with a logseries-abundance distribution with 86 species and a simulation grid side = 256.

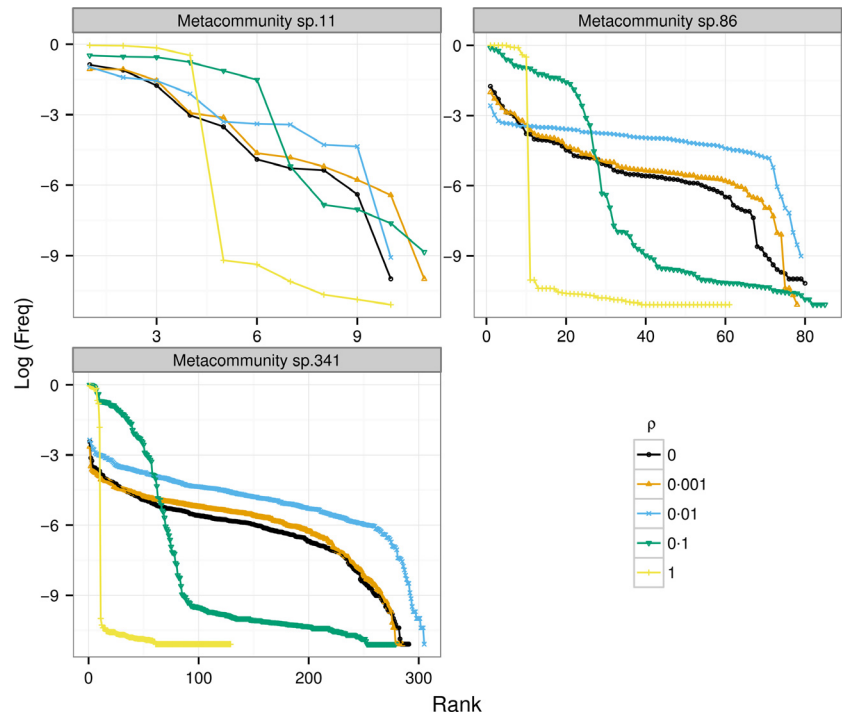


Fig. 5. Rank-abundance diagrams of communities patterns generated with a spatial neutral/hierarchical model with different number of species in the metacommunity (labelled in each subfigure). ρ is the parameter that determines the degree of neutrality. When this parameter is 0, the model is completely neutral and there is no competitive replacement of species. When ρ is 1, competitive superior species always replaces inferior ones and the model is completely hierarchical. The simulations use a metacommunity with a logseries-abundance distribution with 11, 86 and 341 species and a simulation grid side = 256, the other parameters used were mortality rate = 0.2, dispersal distance = 0.4 (2.5 grid units) and colonization rate = 0.001. The ranks were calculated with averages of species densities over 50 simulations.

For communities with lower species numbers (11 species in the metacommunity), the SAD comparisons had a constant low power (Table 4) and also had low power comparing communities with different degree of neutrality (Fig. 8); as the number of points used in the test is the number of species, the power is low thus no matter how different the

communities are. In contrast, the generalized dimensions D_q^{SAD} and D_q^{SRS} had a high power, but type I errors also greater than α . One way to alleviate this problem is to check for a coincidence of the two methods SAD and D_q ; another would be to increase the number of points used inside the q range, because D_q can be calculated for any real number.

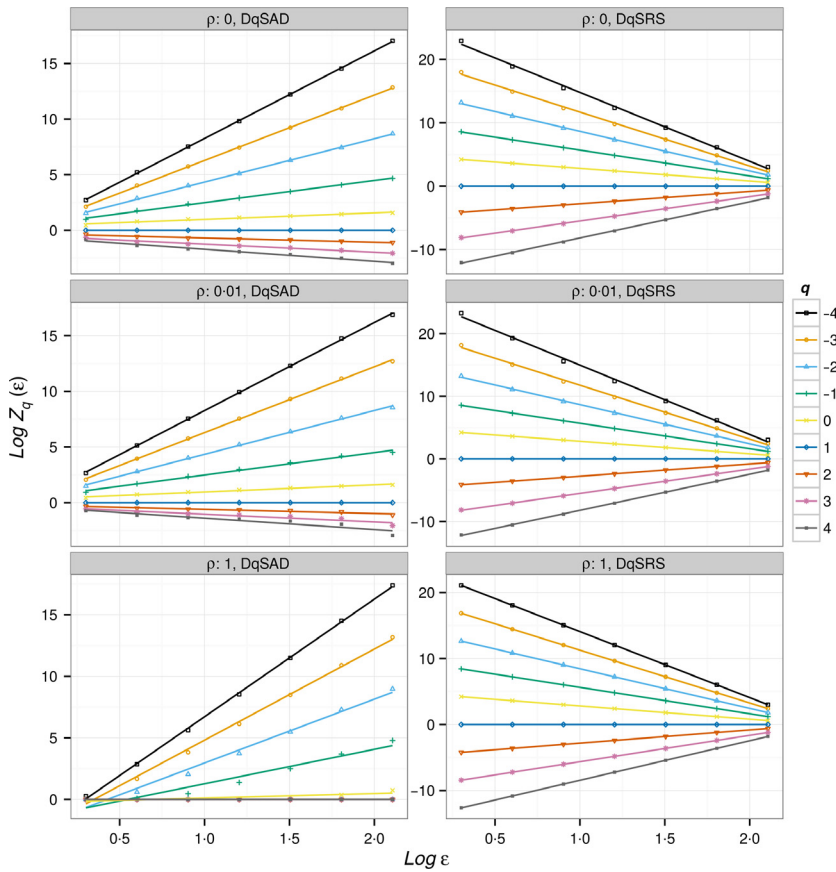


Fig. 6. Linear fit of $Z_q(\epsilon)$ to estimate generalized dimensions (D_q) from spatial patterns generated with a neutral/hierarchical model. Rho (ρ) is the parameter that determines the degree of neutrality. When this parameter is 0, the model is completely neutral and there is no competitive replacement of species. When ρ is 1, competitive superior species always replaces inferior ones and the model is completely hierarchical. *Species* is the number of species actually present plot. The simulations use a metacommunity with a logseries-abundance distribution with 86 species and a simulation grid side = 256 sites.

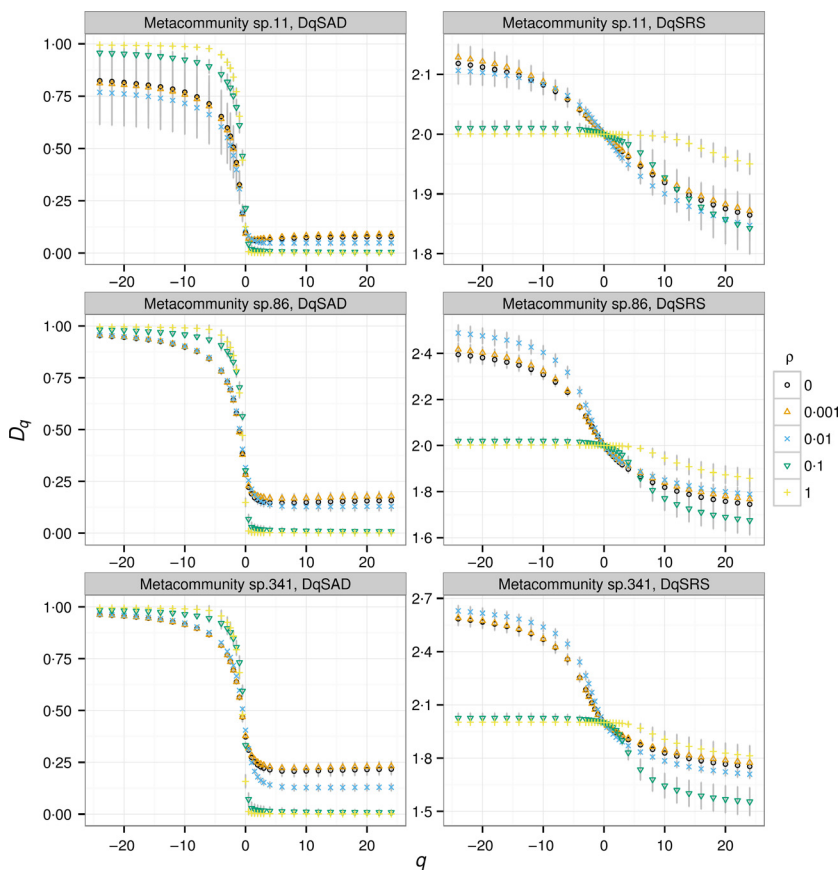


Fig. 7. Generalized dimension spectra D_q of spatial patterns generated with a spatial neutral/hierarchical model. ρ is the parameter that determines the degree of neutrality. When this parameter is 0, the model is completely neutral and there is no competitive replacement of species. When ρ is 1, competitive superior species always replaces inferior ones and the model is completely hierarchical. The points are means, and vertical lines are standard deviation of 50 simulated patterns. Simulations use a metacommunity with a logseries-abundance distribution with 11, 86 and 341 species. The simulation grid side is 256, and the other parameters are given in the main text.

Here I used 21 points (Table 4) but that could be increased, as the only restriction is the additional computational time required. In simulated communities with more species (86 and 341 species metacommunity), the type I error fell below α for all the methods and the overall SAD was slightly more powerful (Table 4).

Differences between communities influence power (Fig. 8). Note that with $\rho < 0.1$, the communities compared are more neutral with a similar number of species and SADs. These cases correspond to the first two rows of Fig. 8; the power in most cases was below 0.5, and thus, D_q^{SAD} and D_q^{SRS} could not discriminate communities. The exception was SAD for neutral communities, where the metacommunity had 341 species, and the power was near or >0.5 . These are comparisons with a higher number of points (~100) resulting in a greater power.

Communities with $\rho \geq 0.1$ are more hierarchical and have different numbers of species and SAD than communities with $\rho < 0.1$. For these cases (last two rows of Fig. 8), the power was high (over 0.75) in most cases. The comparison between more hierarchical communities $\rho \geq 0.1$, is different: SAD and D_q^{SAD} , had less power (below 0.25 in some cases), and D_q^{SRS} had the highest power.

Discussion

In this paper, I present a new macroecological metric D_q^{SRS} based on generalized dimensions and use model simulations to compare it with other similar metrics: D_q^{SAD} , SAD, SAR exponent and information dimension.

While D_q^{SAD} measures the change in SAD with scale, D_q^{SRS} represents the change in the spatial distribution of ranks of species and is thus related to the spatial pattern of species and to their abundance distribution. D_q^{SAD} also reflects changes in spatial pattern, but my results suggest that it cannot distinguish between regular and randomized spatial patterns. In contrast, D_q^{SRS} curves differed clearly between these patterns.

Table 3. Power and type I error rate for *t*-test comparison of a single dimension of the generalized spectra: the SAR exponent (D_0^{SAD}) and information dimension of the species-rank surface (D_1^{SRS}). The test use the standard deviation obtained in the regressions to fit generalized dimensions. The number of comparisons to calculate the power is $n = 25\ 000$ and for type I error $n = 6125$

Side	Metacommunity no. species	Mean no. species	Type	Power	Type I error
512	11	5.96	D_1^{SRS}	0.512	0.434
			D_0^{SAD}	0.498	0.494
	86	36.54	D_1^{SRS}	0.521	0.430
			D_0^{SAD}	0.445	0.426
	341	111.31	D_1^{SRS}	0.497	0.342
			D_0^{SAD}	0.494	0.436
256	11	5.90	D_1^{SRS}	0.491	0.408
			D_0^{SAD}	0.471	0.424
	86	32.27	D_1^{SRS}	0.501	0.447
			D_0^{SAD}	0.474	0.388
	341	76.57	D_1^{SRS}	0.490	0.389
			D_0^{SAD}	0.443	0.363

All D_q curves can be interpreted in terms of q , a parameter that modulates the weight of abundant and rare species in the distribution; D_q for positive q reflects more abundant species, or dominance patterns in SAD, while D_q for negative q represents rare species patterns. An alternative way to analyse D_q would be to split species into ranges of abundances and calculate D_0^{SAD} or D_1^{SRS} . This has been done for biomass and forest height spatial analyses (Seuront & Spilmont 2002; Kellner & Asner 2009), but for species distributions, it has several drawbacks. First, the species' spatial distribution is analysed as a whole, and it is quite possible that the complete set of species fits power laws very well, but one or more single species do not (Šizling & Storch 2004). Secondly, rare species represent a few points in space, and thus, the estimation of D_q will have a high uncertainty. Thirdly, if we replace q by ranges of abundance, the theory developed for D_q would not be valid (Harte 2001).

In neutral models, the SAR exponent depends on speciation rate (in this case migration from a metacommunity), dispersal distance and local community size (Chave, Muller-Landau & Levin 2002; Rosindell & Cornell 2007; Cencini, Pigolotti & Muñoz 2012). I did not expect to find high statistical power using the SAR exponent (D_0^{SAD}) because I did not vary

Table 4. Power and type I error rate of Anderson–Darling statistic to test hypothesis of differences in species-abundance distributions (SAD), generalized dimension based on SAD (D_q^{SAD}) and generalized dimension based on SRS (D_q^{SRS}). The power is calculated testing communities with different ρ , and type I error is calculated for communities with the same ρ . The *P*-values were estimated using 1000 randomizations. The number of points used for SAD comparisons is the number of species found in the communities. The number of points used for multifractal spectra corresponds to the q in the range -10 to 10 ($n = 21$), according to the following set $q = \{-10, -8, -6, -4, -3, -2.5, -2, -1.5, -1, -0.5, 0, 0.5, 1, 1.5, 2, 2.5, 3, 4, 6, 8, 10\}$. The number of comparisons for the power calculations was $n = 25\ 000$ except for SAD with side = 500 and metacommunity species = 11, where some comparison with <3 species was skipped ($n = 23\ 800$). For type I error, the comparisons were $n = 6125$ and the same exception applies ($n = 5846$)

Side	Metacommunity no. species	Mean no. species	Type	Power	Type I error
512	11	5.96	SAD	0.115	0.025
			D_1^{SRS}	0.720	0.102
	86	36.54	D_q^{SAD}	0.568	0.212
			SAD	0.697	0.009
	341	111.31	D_1^{SRS}	0.680	0.014
			D_q^{SAD}	0.616	0.011
256	11	5.90	SAD	0.830	0.039
			D_1^{SRS}	0.688	0.000
	86	32.27	D_q^{SAD}	0.609	0.017
			SAD	0.175	0.000
	341	76.57	D_1^{SRS}	0.654	0.068
			D_q^{SAD}	0.704	0.204
512	11	5.90	SAD	0.675	0.019
			D_1^{SRS}	0.657	0.025
	86	32.27	D_q^{SAD}	0.613	0.027
			SAD	0.799	0.035
	341	76.57	D_1^{SRS}	0.670	0.030
			D_q^{SAD}	0.610	0.048

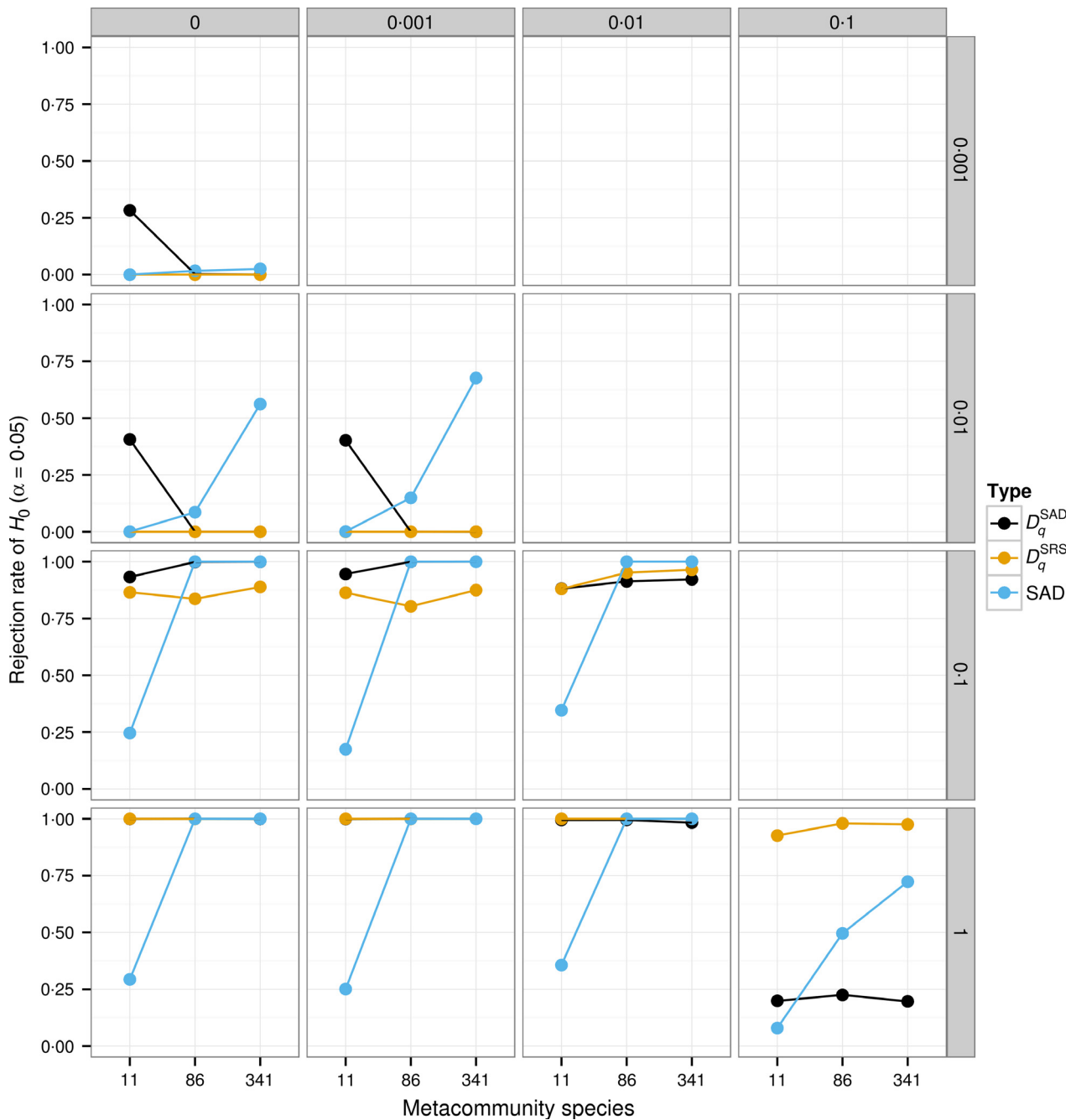


Fig. 8. Power of the Anderson–Darling test for the hypothesis of differences between simulated neutral/hierarchical communities. The test uses generalized dimensions curves calculated from species–abundance distributions (SAD) (D_q^{SAD}), generalized dimensions calculated from the species–rank surfaces (D_q^{SRS}) and the SAD. The compared communities differ only in parameter ρ (across panels) that determines the degree of neutrality/hierarchy. The number of comparisons to calculate the frequency is 2500 in all cases. Simulations use a metacommunity with a logseries–abundance distribution with 11, 86 and 341 species; a grid side of 256 sites, the other parameters are given in the main text.

migration or dispersal and did not make comparisons between different community sizes. But I found high type I error rates for D_0^{SAD} and D_1^{SRS} . This means that the statistical methods should be improved, for instance by applying a correction for autocorrelation to lower type I errors, and using a greater number of boxes. In most cases, a range of different D_q values exists, meaning that the distribution is a multifractal (Stanley & Meakin 1988) and thus will not be well described by only one generalized dimension. To compare communities, D_q^{SRS}

and D_q^{SAD} represent an improvement over comparisons made with such as SAR exponent or information dimension, which use only one dimension.

The SAD is the most studied biodiversity pattern in ecology, but it is generally studied only at one scale. Here I used the whole simulation area, and at this scale, the power of SAD is comparable to that of generalized dimensions. Several studies regard SAD as not very informative because many different models can produce the same patterns (Chave, Muller-Landau

& Levin 2002; Chisholm & Pacala 2010; Rosindell & Cornell 2013), but in my simulations, SAD could differentiate models quite well, except for communities with low richness, where its power was low. Generally, the performance of SAD depends on the number of species used in the comparison. When the number of species is around 100, SAD comparison is the only method that can detect differences between very similar neutral communities.

The analysis comparing competitive hierarchical communities highlights the ability of D_q^{SRS} to detect differences in spatial patterns of rare species. Spatial pattern is interdependent with the shape of SAD; for hierarchical communities, there are few dominant species that form patches with sizes similar to the simulation area, and rare species are scattered. This pattern is enhanced by SRS, and thus, different communities can be detected with high power. For neutral communities, the SAD is more equitable, as there are more species with enough abundances to form species clusters. D_q^{SAD} and D_q^{SRS} thus have a high power to detect differences between neutral communities, except when these communities are very similar. The advantage of D_q over SAD is that the power should be improved by using a greater number of q values, and this possibility should be the subject of future studies.

In summary, D_q^{SRS} always had better fits than D_q^{SAD} and can be applied in all the cases simulated here. It maintained a high power comparing hierarchical communities when the other methods failed. SADs also exhibited good performance, except in a few cases noted above. I note, however, that a better approach could be to use both D_q^{SRS} and SAD, and perhaps add other patterns as well (Münkemüller *et al.* 2012). For these reasons, this new macroecological metric could be a valuable addition to the already established ones and should be used in the study of the scaling of SAD.

Acknowledgements

I am grateful to the National University of General Sarmiento for financial support, to Graeme Ruxton and Ben Bond-Lamberty for their English revisions.

Data accessibility

All data and R scripts used in this manuscript are available at figshare <http://dx.doi.org/10.6084/m9.figshare.1276105>.

References

- Anand, M. & Langille, A. (2010) A model-based method for estimating effective dispersal distance in tropical plant populations. *Theoretical Population Biology*, **77**, 219–226.
- Beck, C. (1990) Upper and lower bounds on the Renyi dimensions and the uniformity of multifractals. *Physica D: Nonlinear Phenomena*, **41**, 67–78.
- Borda-de-Água, L., Hubbell, S.P. & He, F. (2007) Scaling biodiversity under neutrality. *Scaling Biodiversity* (eds D. Storch, P.A. Marquet & J.H. Brown), pp. 347–375. Cambridge University Press, Cambridge.
- Borda-de-Água, L., Hubbell, S.P. & McAllister, M. (2002) Species-area curves, diversity indices, and species abundance distributions: a multifractal analysis. *American Naturalist*, **159**, 138–155.
- Cencini, M., Pigolotti, S. & Muñoz, M.A. (2012) What ecological factors shape species-area curves in neutral models? *PLoS One*, **7**, e38232.
- Chappell, D. & Scalo, J. (2001) Multifractal scaling, geometrical diversity, and hierarchical structure in the cool interstellar medium. *Astrophysical Journal*, **551**, 712–729.
- Chave, J., Muller-Landau, H.C. & Levin, S.A. (2002) Comparing classical community models: theoretical consequences for patterns of diversity. *American Naturalist*, **159**, 1–23.
- Chisholm, R.A. & Pacala, S.W. (2010) Niche and neutral models predict asymptotically equivalent species abundance distributions in high-diversity ecological communities. *Proceedings of the National Academy of Sciences*, **107**, 15821–15825.
- Condit, R., Pitman, N. Jr, Leigh, E.G., Chave, J., Terborgh, J. *et al.* (2002) Beta-diversity in tropical forest trees. *Science*, **295**, 666–669.
- Crawley, M.J. & Harral, J.E. (2001) Scale dependence in plant biodiversity. *Science*, **291**, 864–868.
- Dal Bello, M., Maggi, E., Rindi, L., Capocchi, A., Fontanini, D. *et al.* (2014) Multifractal spatial distribution of epilithic microphytobenthos on a Mediterranean rocky shore. *Oikos*, **124**, 477–485.
- Edgington, E. (1995) *Randomization Tests*, 3rd edn. CRC Press, New York, USA.
- Etienne, R.S. (2007) A neutral sampling formula for multiple samples and an “exact” test of neutrality. *Ecology Letters*, **10**, 608–618.
- Evertsz, C.J.G. & Mandelbrot, B.B. (1992) Multifractal measures. *Chaos and Fractals: New Frontiers of Science* (eds H.-O. Peitgen, H. Jurgens & D. Saupe), pp. 921–953. Springer, New York, USA.
- Feigelson, E.D. & Babu, G.J. (2012) *Modern Statistical Methods for Astronomy: with R Applications*. Cambridge University Press, Cambridge.
- Fisher, R.A., Corbet, A.S. & Williams, C.B. (1943) The relation between the number of species and the number of individuals in a random sample of an animal population. *Journal of Animal Ecology*, **12**, 42–58.
- Gamarra, J.G.P. (2005) Metapopulations in multifractal landscapes: on the role of spatial aggregation. *Proceedings of the Royal Society London Series B*, **272**, 1815–1822.
- Grassberger, P. (1983) Generalized dimensions of strange attractors. *Physics Letters A*, **97**, 227–230.
- Gravel, D., Canham, C.D., Beaudet, M. & Messier, C. (2006) Reconciling niche and neutrality: the continuum hypothesis. *Ecology Letters*, **9**, 399–409.
- Hankin, R.K.S. (2007) Introducing untb, an R package for simulating ecological drift under the unified neutral theory of biodiversity. *Journal of Statistical Software*, **22**, 1–15.
- Harte, D. (2001) *Multifractals: Theory and Applications*. Chapman & Hall/CRC, Boca Raton.
- Hentschel, H.G.E. & Procaccia, I. (1983) The infinite number of generalized dimensions of fractals and strange attractors. *Physica D: Nonlinear Phenomena*, **8**, 435–444.
- Hill, M.O. (1973) Diversity and evenness: a unifying notation and its consequences. *Ecology*, **54**, 427–432.
- Hubbell, S.P. (2001) *The Unified Neutral Theory of Biodiversity and Biogeography*. Princeton University Press. Available: <http://books.google.com.ar/books?id=EIQpFBu84NoC>.
- Kellner, J.R. & Asner, G.P. (2009) Convergent structural responses of tropical forests to diverse disturbance regimes. *Ecology Letters*, **12**, 887–897.
- Kirkpatrick, L.A. & Weishampel, J.F. (2005) Quantifying spatial structure of volumetric neutral models. *Ecological Modelling*, **186**, 312–325.
- Kutner, M., Nachtsheim, C., Neter, J. & Li, W. (2005) *Applied Linear Statistical Models*, 5 edn. McGraw-Hill/Irwin, New York.
- Laurie, H. & Perrier, E. (2011) Beyond species area curves: application of a scale-free measure for spatial variability of species richness. *Oikos*, **120**, 966–978.
- Legendre, P., Dale, M.R.T., Fortin, M.J., Gurevitch, J., Hohn, M. *et al.* (2002) The consequences of spatial structure for the design and analysis of ecological field surveys. *Ecography*, **25**, 601–615.
- Liebovitch, L.S. (1998) *Fractals and Chaos Simplified for the Life Sciences*. Oxford University Press, Oxford.
- McGill, B.J., Etienne, R.S., Gray, J.S., Alonso, D., Anderson, M.J., *et al.* (2007) Species abundance distributions: moving beyond single prediction theories to integration within an ecological framework. *Ecology Letters*, **10**, 995–1015.
- Molofsky, J. & Bever, J.D. (2004) A new kind of ecology? *BioScience*, **54**, 440–446.
- Münkemüller, T., de Bello, F., Meynard, C.N., Gravel, D., Lavergne, S. *et al.* (2012) From diversity indices to community assembly processes: a test with simulated data. *Ecography*, **35**, 468–480.
- Newman, M.E.J. (2005) Power laws, Pareto distributions and Zipf's law. *Contemporary Physics*, **46**, 323–351.
- Preston, F.W. (1960) Time and space and the variation of species. *Ecology*, **41**, 612–627.
- R Core Team. (2014) *R: A Language and Environment for Statistical Computing*. R Foundation for Statistical Computing, Vienna, Austria. URL: <http://www.r-project.org/>.

- Renyi, A. (1970) *Probability Theory*. North-Holland, Amsterdam, the Netherlands.
- Ricotta, C. (2000) From theoretical ecology to statistical physics and back: self-similar landscape metrics as a synthesis of ecological diversity and geometrical complexity. *Ecological Modelling*, **125**, 245–253.
- Rosindell, J. & Cornell, S.J. (2007) Species–area relationships from a spatially explicit neutral model in an infinite landscape. *Ecology Letters*, **10**, 586–595.
- Rosindell, J. & Cornell, S.J. (2013) Universal scaling of species-abundance distributions across multiple scales. *Oikos*, **122**, 1101–1111.
- Rosindell, J., Hubbell, S.P. & Etienne, R.S. (2011) The unified neutral theory of biodiversity and biogeography at age ten. *Trends in Ecology & Evolution*, **26**, 340–348.
- Saravia, L.A. (2014) mfsBA: multifractal analysis of spatial patterns in ecological communities [v2; ref status: indexed, <http://f1000r.es/347>]. *F1000Research*, **3**, 14.
- Saravia, L.A., Giorgi, A. & Momo, F. (2012a) Multifractal growth in periphyton communities. *Oikos*, **121**, 1810–1820.
- Saravia, L.A., Giorgi, A. & Momo, F.R. (2012b) Multifractal spatial patterns and diversity in an ecological succession. *PLoS One*, **7**, e34096.
- Scheuring, I. & Riedi, R.H. (1994) Application of multifractals to the analysis of vegetation pattern. *Journal of Vegetation Science*, **5**, 489–496.
- Scholz, F.W. & Stephens, M.A. (1987) K-Sample Anderson-Darling Tests. *Journal of the American Statistical Association*, **82**, 918–924.
- Scholz, F. & Zhu, A. (2012) kSamples: K-sample rank tests and their combinations. URL: <http://cran.r-project.org/package=kSamples>.
- Seuront, L. (2009) *Fractals and Multifractals in Ecology and Aquatic Science*. Taylor & Francis, Boca Raton.
- Seuront, L. & Spilmont, N. (2002) Self-organized criticality in intertidal microphytobenthos patch patterns. *Physica A*, **313**, 513–539.
- Seuront, L. & Stanley, H.E. (2014) Anomalous diffusion and multifractality enhance mating encounters in the ocean. *Proceedings of the National Academy of Sciences*, **111**, 2206–2211.
- Šizling, A.L. & Storch, D. (2004) Power-law species–area relationships and self-similar species distributions within finite areas. *Ecology Letters*, **7**, 60–68.
- Šizling, A.L., Kunin, W.E., Šizlingová, E., Reif, J. & Storch, D. (2011) Between geometry and biology: the problem of universality of the species–area relationship. *The American Naturalist*, **178**, 602–611.
- Stanley, H.E. & Meakin, P. (1988) Multifractal phenomena in physics and chemistry. *Nature*, **335**, 405–409.
- Tilman, D. (1994) Competition and biodiversity in spatially structured habitats. *Ecology*, **75**, 2–16.
- Tjørve, E. (2003) Shapes and functions of species–area curves: a review of possible models. *Journal of Biogeography*, **30**, 827–835.
- Wei, S.-G., Li, L., Huang, Z.-L., Ye, W.-H., Gong, G.-Q. *et al.* (2013) Multifractal analysis of diversity scaling laws in a subtropical forest. *Ecological Complexity*, **13**, 1–7.
- White, E.P., Ernest, S.K.M., Adler, P.B., Hurlbert, A.H. & Lyons, S.K. (2010) Integrating spatial and temporal approaches to understanding species richness. *Philosophical Transactions of the Royal Society of London Series B*, **365**, 3633–3643.
- Yakimov, B.N., Bossuyt, B., Iudin, D.I. & Gelashvili, D.B. (2008) Multifractal diversity–area relationship at small scales in dune slack plant communities. *Oikos*, **117**, 33–39.
- Yakimov, B.N., Iudin, D.I., Solntsev, L.A. & Gelashvili, D.B. (2014a) Multifractal analysis of neutral community spatial structure. *Journal of Theoretical Biology*, **343**, 44–53.
- Yakimov, B.N., Gelashvili, D.B., Solntsev, L.A., Iudin, D.I. & Rozenberg, G.S. (2014b) Nonconcavity of mass exponents' spectrum in multifractal analysis of community spatial structure: the problem and possible solutions. *Ecological Complexity*, **20**, 11–22.
- Zhang, Y., Ma, K., Anand, M. & Fu, B. (2006) Do generalized scaling laws exist for species abundance distribution in mountains? *Oikos*, **115**, 81–88.

Received 31 March 2015; accepted 26 May 2015

Handling Editor: Tamara Münkemüller

Supporting Information

Additional Supporting Information may be found in the online version of this article.

Appendix S1. Model Description.

Appendix S2. Additional tables and figures.